Journal of Hazardous Materials 185 (2011) 1311–1317

Contents lists available at ScienceDirect

Journal of Hazardous Materials

journal homepage: www.elsevier.com/locate/jhazmat

Removal of Cu(II) from water by tetrakis(4-carboxyphenyl) porphyrin-functionalized mesoporous silica

Eun-Young Jeong, Mohd Bismillah Ansari, Yong-Hwan Mo, Sang-Eon Park*

Laboratory of Nano-Green Catalysis and Nano Center for Fine Chemical Fusion, Technology, Department of Chemistry, Inha University, Incheon, 402-751, Republic of Korea

ARTICLE INFO

Article history:
Received 23 July 2010
Received in revised form
17 September 2010
Accepted 11 October 2010
Available online 19 October 2010

Keywords:
Copper ion adsorbent
Tetrakis(4-carboxyphenyl)porphyrin
Hybrid nanoporous materials

ABSTRACT

Various adsorbents are available for the removal of heavy and toxic metals, silica-based materials have been the most popular. Recently, there has been considerable interest for the modification of organic moieties and mesostructured materials to enable their use as efficient adsorbent for metal removal. In this study, here we are reporting successful incorporation of tetrakis(4-carboxyphenyl)porphyrin (TCPP) in mesoporous silica by the post-synthetic method. TCPP-SBA-15 has been found to be an effective material for the removal of Cu(II) from aqueous solution due to the chelating nature of the porphyrin-bridging group. A comparative study on adsorption of copper(II) ion over NH_2-SBA-15 silica and TCPP-SBA-15 was performed. The results show that TCPP-SBA-15 material has higher adsorption capacity than NH_2-SBA-15 silica and it reaches the adsorption maxima around 13 mmol g^{-1}.

1. Introduction

Since several decades, numerous environmental problems have been caused by the discharge of heavy metals from chemical, electronics, metallurgical and machine manufacturing industries contaminating soil and water [1,2]. Among environmental problem, water pollution by heavy metals is a serious environmental problem, resulting in the progress of research aimed at its decrease or elimination and recovery of waste by various means.

Heavy metals, which exert serious toxic effects on human beings [3], are difficult to eliminate and are also absorbed by aquatic animals and plants as well as agricultural crops; these metals ultimately enter the human body through the food chain [4]. In particular, Cu(II) is one of the hazardous metal ions present in wastewater discharge and effluent from many industries [5]. The existence of a Cu(II) imbalance in the body can cause headaches, fatigue, insomnia, depression, skin rashes, spaciness or detachment, learning disorders, or premenstrual syndrome, and it can even lead to accumulation in the kidneys, brain, skin, pancreas, and heart.

Conventional methods for the removal of heavy metal ions in aqueous solutions include chelation therapy, chemical treatment, ion exchange, electrolysis, adsorption, reverse osmosis, electrodialysis, and biological treatment [6–11]. Several studies have shown that the efficiency of removing heavy metals from wastewater by adsorption method, were dependent on physical and chemical composition of the adsorbents because of its simplicity, relatively low cost, and effectiveness in removing heavy metal ions from water.

Sarl et al. [12] reported the adsorption of Pb(II) and Cr(III) from aqueous solution on Celtek clay. Studies have concluded that the Celtek clay can successfully be used for the removal of metal using adsorption method. Utilization of Celtek clay has a major advantage of low cost recovery processes making them appropriate for use in water purification. Sönmez et al. [13] studied the removal of Cu(II) in polypyrrole–chloride. This adsorbent showed a high selectivity over Cu(II) ions in the pH range of 4–7.

Ordered mesoporous silica materials are one of the most extensively used adsorbents for trapping pollutants [14,15]. Recently, organic–inorganic hybrid adsorbents have been developed. In addition, many studies have focused on developing nanostructured materials, particularly ordered organic–inorganic hybrid materials with mesoporosity. Because ordered mesoporous silicas have many advantages such as good accessibility to active sites [16], rapid mass transport inside the nanostructures [17], and good hydrothermal stability [18]. In addition, mesoporous silica materials can be readily modified with organic groups such as mercaptopropyl [19], propylamine [20], aminopropyl [21], imidazole [22], cyclam [23], to tune their characteristics for effective metal removal. In this context, Porphyrins have gained particular interest as a ligand for metal removal because of their high metal removal efficiency [24] and ligational properties. The nitrogen atoms in the tetrapyrrole ring act as ligational sites and also attract metal ions on account of their strong electron-donor properties, thus providing a high

* Corresponding author. Tel.: +82 32 860 7675; fax: +82 32 872 8670.
E-mail address: separk@inha.ac.kr (S.-E. Park).

0304-3894/$ – see front matter © 2010 Elsevier B.V. All rights reserved.
doi:10.1016/j.jhazmat.2010.10.047

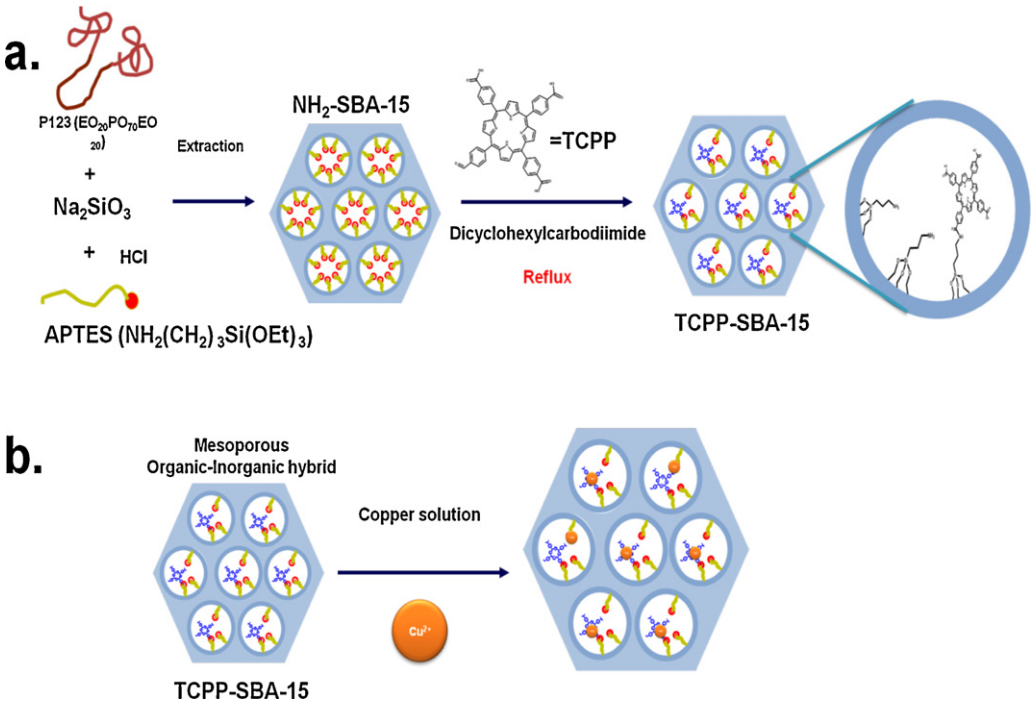

Scheme 1. Illustration of tetrakis(4-carboxyphenyl)porphyrin(TCPP) immobilized amino functionalized SBA-15 (a) and Cu(II) binding to TCPP grafted silica.

removal efficiency via the formation of metal–nitrogen coordination bonds.

In this paper, we report TCPP immobilized NH_2-SBA-15(TCPP-SBA-15) as a metal ion adsorbent. Amino-functionalized SBA-15 (NH_2-SBA-15) was synthesized directly from the co-condensation of sodium metasilicate and aminopropyltriethoxysilane (APTES) (Scheme 1a). TCPP functionalized NH_2SBA-15 were prepared by using post synthesis method (denoted as TCPP-SBA-15) (Scheme 1a), their performances for the adsorption of Cu(II)-ions evaluated (Scheme 1b).

The immobilization of TCPP on NH_2-SBA-15 was attributed to the following reasons. (i) The amino group on SBA-15 can easily react with the carboxyl acid group of TCPP. (ii) TCPP plays the role of a metal remover. (iii) The presence of free amino groups on the support enhances the metal removal ability because the amino groups which can coordinate to the metal ion. In order to evaluate the metal adsorption capacity of TCPP-functionalized SBA-15 (TCPP-SBA-15), demetallation experiments were performed at different Cu(II) ion concentrations. The distribution coefficients associated with Cu(II) adsorption on TCPP-SBA-15 were also determined.

2. Materials and methods

2.1. Reagents and materials

The amino-functionalized SBA-15 was synthesized according to our previous work [25]. Pyrrole and 4-carboxybenzaldehyde and propionic acid were purchased from Sigma–Aldrich Corporation, St. Louis, MO, USA. Other chemicals for synthesizing materials and testing catalytic activity were purchased from Sigma–Aldrich and directly used without further purification

2.2. Synthesis of tetrakis(4-carboxyphenyl)porphyrin (TCPP)

Pyrrole (2.33 mmol) and 4-carboxybenzaldehyde (2.33 mmol) were dissolved in 100 mL propionic acid. And the mixture was refluxed for 4 h, and then this crude product was cool to room temperature. After cooling to room temperature, the mixture was added to 100 mL of methanol and chilled in an ice bath with stirring. The deep-purple crystals are filtered and washed with methanol and hot water. The resulting solid was dissolved in chloroform containing 2% acetone and purified by column chromatography over silica gel using chloroform as eluent.

2.3. Synthesis of tetrakis(4-carboxyphenyl) porphyrin-functionalized mesoporous silica

In a round bottom flask, 1.0 g of amino functionalized SBA-15 and 0.18 g dicyclohexylcarbodiimide (DCHC) were suspended in 50 mL of N,N-dimethylformamide (DMF). The 0.88 mmol of tetrakis(4-carboxyphenyl)porphyrin was dissolved in 5 mL of DMF and added drop wise to round bottom flask. The mixture was refluxed at 60 °C for 8 h. After cooling down to room temperature, the product was filtered and dried.

2.4. Characterization

The XRD patterns were obtained by using a rigaku multiflex diffractometer with a monochromated high-intensity Cu Kα radiation (λ = 1.54 Å). Scanning was performed under ambient conditions over the 2θ region of 0.7–5° at the rate of 0.1°/min (20 kV, 10 mA). The N_2 adsorption–desorption isotherms and pore characterization were obtained by using a Micromeritics ASAP 2020 apparatus at liquid N_2 temperature. Pore distributions were calculated by using BJH method from the adsorption branches. The scanning electron microscope (SEM) images were observed using a JEOL 630-F microscope. Before the measurement, the samples were dispersed onto a steel plate surface and coated with Pt metal. Transmission electron microscope (TEM) images were observed using a JEM-2100F instrument (JEOL). Metal concentration were measured using Inductively Coupled Plasma Spectrometer (Optima 7300DV). Thermogravimetric analysis (Bruker 2010SA) were carried out to detect the decomposition temperature of the organic moieties grafted on the mesoporous silica. Samples were heated from room temperature to 900 °C at the heating rate of 10 °C/min.

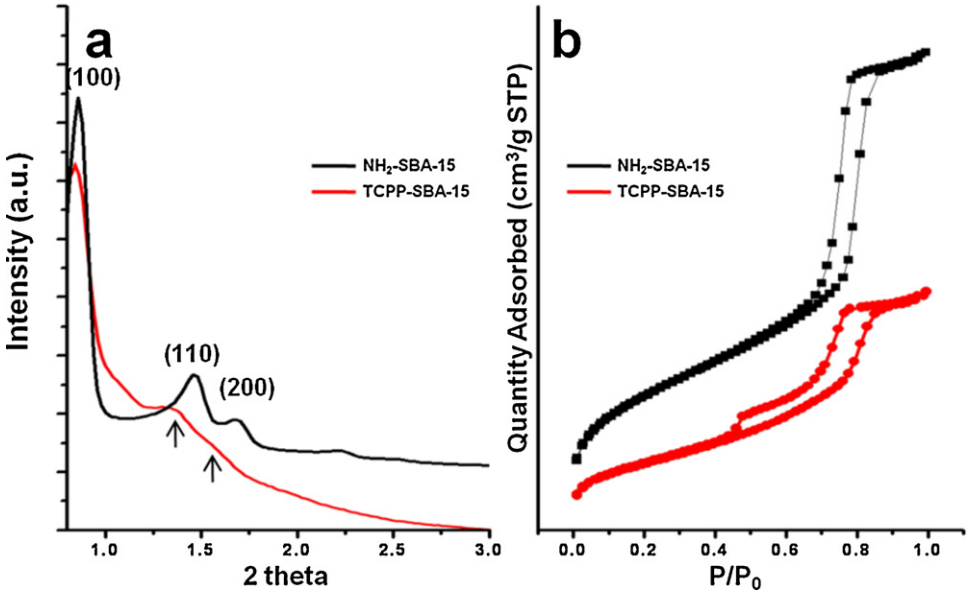

Fig. 1. (a) Powder XRD patterns and (b) N_2 adsorption–desorption isotherms of NH_2-SBA-15 and TCPP-SBA-15.

The tetrakis(4-carboxyphenyl)porphyrin were analyzed by FT-IR (Nicolet) and UV–vis–NIR spectroscopy (SolidSpec-3700).

2.5. Adsorption test

Demetallation experiments was carried out by stirring 100 mg of TCPP-SBA-15 in 250 mL of a metal solution at 25 °C. Two different Cu^{2+} concentrations viz. 1065 and 65 mg L^{-1} were performed. NH_2-SBA-15 was also conducted the same adsorption test. The solution from each vial was analyzed for Cu^{2+} concentration after different time intervals and removal rate of Cu^{2+} was calculated using Eq. (1).

$$Q_e = \frac{C_0 - C_e\, V}{m} \quad (1)$$

where Q_e is quantity of Cu^{2+} adsorbed on the TCPP-SBA-15 at the time of equilibrium (mg/g), C_0 is initial concentration of Cu^{2+} in aqueous solution of $CuSO_4{\cdot}5H_2O$ (mg L^{-1}), and C_e is final concentration of Cu^{2+} in aqueous solution of $CuSO_4{\cdot}5H_2O$ at the time of equilibrium (mg L^{-1}), V is total volume of the solution (L); m mass of adsorbents (g). The distribution coefficient, K_d, for evaluating the affinity of the adsorbent for adsorbate in aqueous solution can be calculated using Eq. (2) [26].

$$K_d = \frac{Q_e}{C_e} \quad (2)$$

3. Results and discussion

The powder low angle X-ray diffraction patterns of NH_2-SBA-15 and TCPP-SBA-15 are shown in Fig. 1a. All the samples showed three well-resolved diffraction peaks, with a very intense peak at 2θ of 0.9–1.18° and two peaks with at 2θ of 1.4–1.8°. These peaks could be indexed to the (1 0 0), (1 1 0), and (2 0 0) planes, which correspond to a mesostructure of hexagonal space group symmetry *p6mm*. The XRD pattern of TCPP-SBA-15 show strong (1 0 0) peaks, which suggests the framework stability of the mesoporous material, is well maintained when the TCPP is functionalized on the NH_2-SBA-15. The relative intensities of the (1 1 0) and (2 0 0) peaks in the TCPP-SBA-15 pattern were lower than those in the NH_2-SBA-15, thereby indicating that the porphyrins are dispersed in the mesoporous channels. Nitrogen adsorption–desorption isotherms for all materials were found to be type IV curve, with well-defined capillary condensation step, characteristic of uniform mesoporous materials (Fig. 1b). The surface area is evaluated from nitrogen adsorption isotherms by using the BET equation. Pore size was calculated by the Barrett–Joyner–Halenda (BJH) method using desorption branch of the adsorption–desorption isotherms. Specific surface areas and mesopore diameters for NH_2-SBA-15 and TCPP-SBA-15 are shown in Table 1. The tendencies of mesopore shrinkage with incorporation TCPP is exhibited by changes in the surface area and total pore volume, which indicate get worse mesostructural features with loading of TCPP groups.

Fig. 2 shows (a, b) scanning electron microscopy (SEM) images and (c, d) transmission electron microscopy (TEM) images of the obtained TCPP-SBA-15. The SEM images reveal shorter channel lengths and hexagonal disk-shape morphology. The TEM images indicate that the lengths of the mesopore channels were in the submicrometer range and that the channel directions of the 2D-hexagonal structures were parallel to the thickness direction of the hexagonal platelet morphology. The short channeled platelet morphology has several advantages, in comparison to conventional SBA-15 having fiber morphology and long mesochannels. The short channeled TCPP-SBA-15 can overcome limitations like mass transfer, accessibility, and diffusion more over short channeled serve for facile adsorption and desorption of Cu(II) ions.

The incorporation of TCPP into mesoporous silica was confirmed by Fourier-transform infrared (FT-IR) spectroscopy (Fig. 3). In the FT-IR spectrum of NH_2-SBA-15, the peaks around 1628 cm^{-1} were assigned to asymmetric NH_2 stretching ($\nu_{as}NH_2$) and NH_2 deformation (δNH_2) [27], and that broad peak at 3300 cm^{-1} could be attributed to the overlap between secondary amine (NH) stretching (νNH) and symmetric NH_2 stretching ($\nu_s NH_2$). The FT-IR spectrum

Table 1
Physicochemical Properties for NH_2-SBA-15 and TCPP-SBA-15.

Sample	S^a ($m^2\,g^{-1}$)	D^b (nm)	V^c ($cm^3\,g^{-1}$)
NH_2-SBA-15	908	8	1.41
TCPP/NH_2-SBA-15	453	7.73	0.70

[a] The surface area is evaluated from nitrogen adsorption isotherms by using the BET equation.
[b] Pore size diameter calculated by the BJH method.
[c] Total pore volume registered at $P/P_0 = 0.995$.

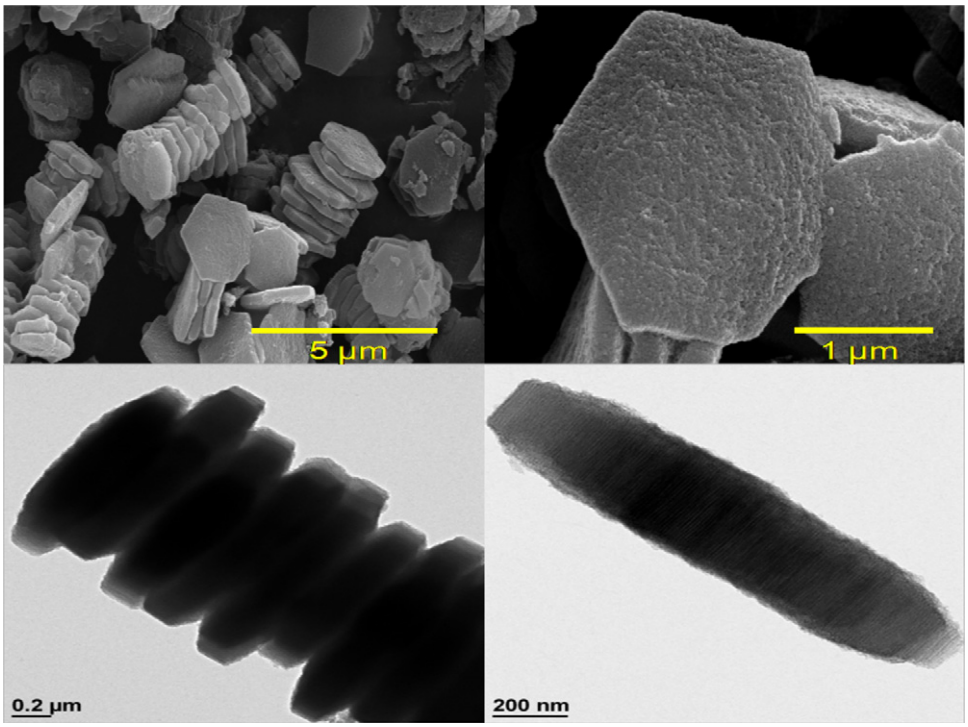

Fig. 2. SEM images (upper picture) and TEM image (bottom picture) of samples TCPP-SBA-15.

of TCPP-SBA-15 revealed peaks at 1713 and 1527 cm^{-1}. These peaks were assigned to the C=O stretching vibration of TCPP and the NH_2 deformation (δNH_2) of the amide group, respectively. The amide group is formed when the carboxyl acid group of TCPP reacts with the amino group on SBA-15. OH stretching of the carboxyl acid group of TCPP (3645 cm^{-1}), overtone of Si–O–Si lattice vibration (1984 and 1850 cm^{-1}), and CH_2 stretching (2863 and 2929 cm^{-1}) were also observed in this spectrum.

The presence of TCPP on SBA-15 was also confirmed by UV–vis spectroscopy (Fig. 4). The TCPP spectrum showed Soret band (417 nm) and four weak Q-bands. TCPP-SBA-15 showed absorption bands at 414 nm (Soret band) and at 514, 548, 591, and 647 nm. This result suggests that TCPP was functionalized onto SBA-15 (as characterized by a blue shift of the Soret band associated with a significant amount of TCPP) during the preparation process. When TCPP was functionalized onto SBA-15, the polarity in the vicinity of TCPP increases, as evidenced by the shifts of the absorption bands towards a higher energy.

After the demetallation reaction, TCPP-SBA-15 was separated and washed. After washing, UV–vis spectroscopic studies were conducted. The UV–vis spectrum of TCPP-SBA-15 containing adsorbed Cu(II) ions is similar to that of Cu-TCPP, which shows a Soret band at 417 nm and two Q-bands at 540 and 583 nm. It is thus observed that Cu molecules were chelated with central nitrogen ligands in TCPP.

An adsorption experiment was performed to investigate the effect of TCPP on the mesoporous silica at different Cu(II) ion concentrations (between 65 and 1065 mg L^{-1}). Comparative experiment was carried out the same condition for the mesoporous silica

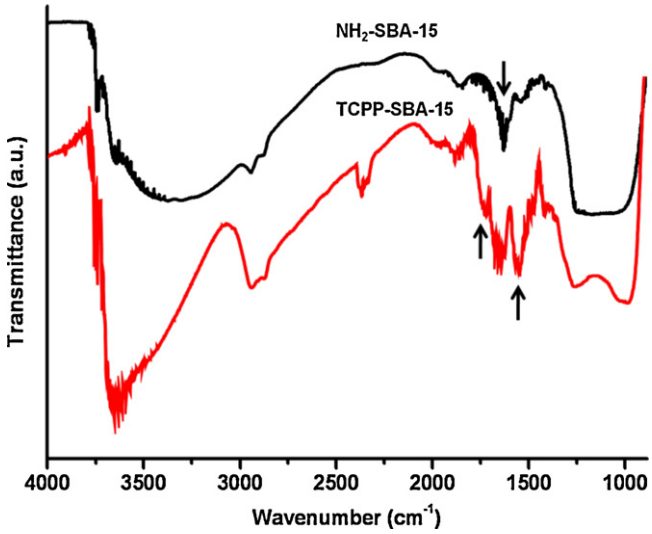

Fig. 3. FT-IR spectra of samples NH_2-SBA-15 and TCPP-SBA-15.

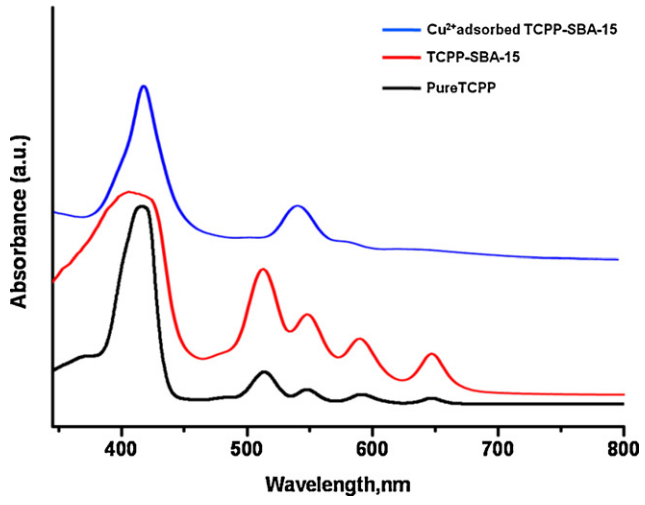

Fig. 4. UV–vis spectra of samples TCPP, TCPP-SBA-15 and Cu(II) adsorbed TCPP-SBA-15.

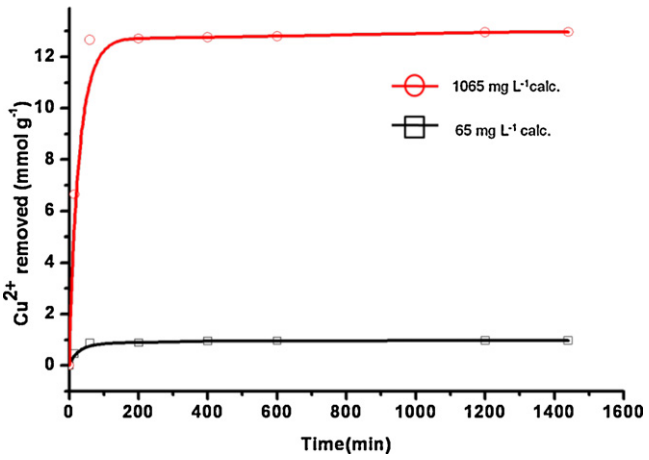

Fig. 5. Adsorption isotherms of Cu(II) on TCPP-SBA-15 with different initial concentration.

without TCPP. The adsorption rate has been analyzed using Eq. (1) and plotted in Fig. 5. The Cu(II) concentration was increased from 65 to 1065 mg L^{-1} in order to attain the plateau values representing the saturation of the active points which are available for interaction with metal ions on TCPP-SBA-15; in other words, the Cu(II) concentration was increased in order to obtain the maximum removal capacities for the metal ions of interest. The maximum adsorption of Cu(II) on the TCPP-SBA-15 sample was 13 mmol of Cu(II) per gram of the adsorbent (Table 2). In addition, high removal rates were observed at the beginning of the experiment, after which equilibrium values were gradually attained within 60 min. Demetallation experiments are usually completed within 1 h, which indicates that the binding process is considerably rapid. This high adsorption capacity was accomplished by the incorporation of porphyrin groups into the silica structure (Fig. 5). As noted earlier, the chelating properties of the porphyrin-bridging group affect the process of metal removal in water. The high affinity of the porphyrin group towards Cu(II) ions resulted in a very high adsorption capacity. The high sorption rates can also be attributed to the uniform porous structure of the material, as characterized by the presence of regular mesochannels.

The efficiency of the TCPP-SBA-15 was also studied towards a waste water sample collected from car paint industry, initially the effluent sample contains 32 mg L^{-1} of Cu^{2+} ion within a short time period of 15 min the concentration of the Cu^{2+} have been reduced to half (15 mg L^{-1}). It is found that after 200 min no Cu^{2+} was observed in the effluent sample as suggested by the ICP-MS studies. Therefore it can be considered as effective system for removal of copper.

The distribution coefficient (K_d) is used for evaluating the affinity of the adsorbent towards Cu(II) ions. The distribution coefficients are summarized in Table 2. In the case of TCPP-SBA-15, K_d increases, indicating that the affinity towards Cu(II) ions increases with the loading of TCPP groups. The fact that the considerable affinity of TCPP groups towards Cu(II) species gives rise to the high distribution coefficient is important from the environmental perspective. The removal capacities of Cu(II) ions at different initial concentrations, as calculated by Eq. (3), are also listed in Table 2.

$$\text{removal capacity}\,(\%) = \frac{(C_0 - C_e)}{C_0} \times 100 \quad (3)$$

The recovery of Cu(II) and regeneration of the adsorbent are key processes. In order to perform these two processes and to measure the practical utility of the adsorbent, desorption experiments were carried out by treating 0.1 g of TCPP-SBA-15 containing adsorbed Cu^{2+} ions with 50 mL of 0.2 M HCl solution over a period of 1 h. Since 0.2 M HCl solution was used, H^+ could replace the metal ions adsorbed by TCPP-SBA-15. Fig. 6 shows the desorption rate of TCPP-SBA-15–metal ion complexes as a function of time. The desorption process reached equilibrium at 60 min and the desorption rate was 65.1% for Cu(II) (Fig. 6a).

Reusability experiments were performed on TCPP-SBA-15 using the same procedure as that followed in the adsorption experi-

Table 2
Cu^{2+} adsorption capacity and distribution coefficient over NH_2-SBA-15 and TCPP-SBA-15.

Sample	C_0 (mg L^{-1})	Q_{max} (mmol g^{-1})	K_d maximum[a]	Removal rate of Cu^{2+} (%)
NH_2-SBA-15	65	0.86	0.28	84
	1065	4.15	13.62	24
TCPP-SBA-15	65	0.97	8.54	95
	1065	12.96	44	77

[a] K_d = distribution coefficient.

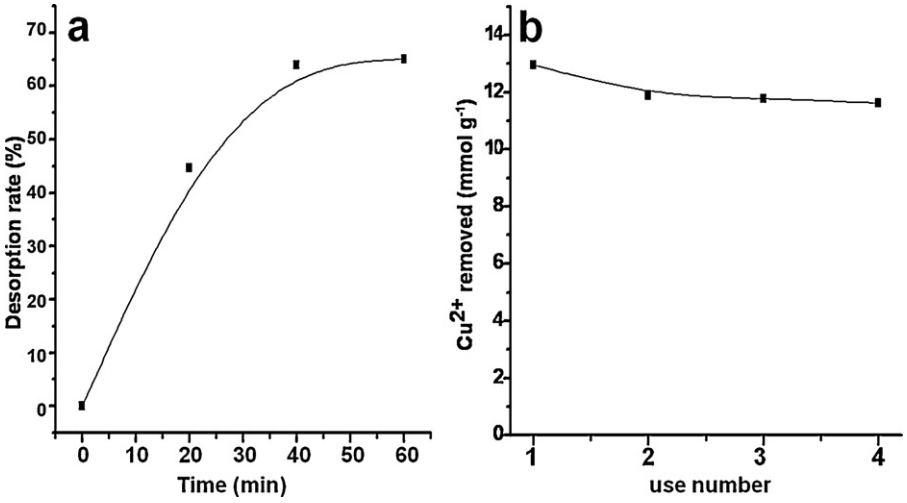

Fig. 6. Desorption rate of Cu(II) from TCPP-SBA-15 (a) and reusability of TCPP-SBA-15 (b).

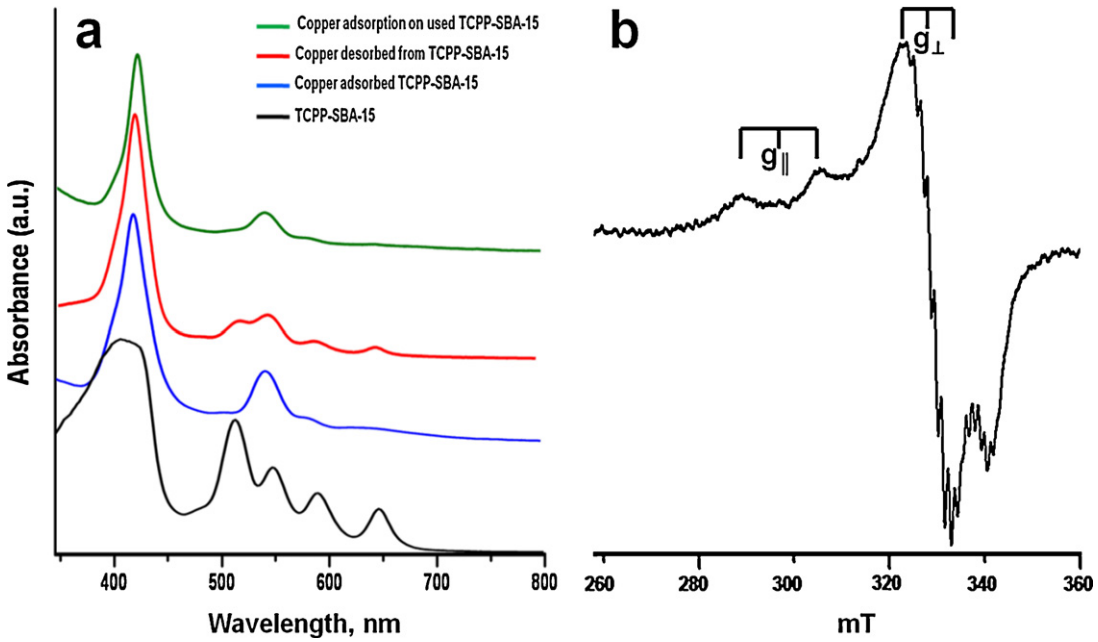

Fig. 7. UV–vis spectroscopy of TCPP-SBA-15, Cu(II) adsorbed TCPP-SBA-15 and Cu(II) desorbed TCPP-SBA-15, regeneration by Cu(II) adsorption on used TCPP-SBA-15 (a) and EPR spectrum of Cu(II) adsorbed TCPP-SBA-15 (b).

ments. Adsorption–desorption cycles were repeated 3 times using the same material (Fig. 6b). The adsorption capacities were found to be around 11.906 mmol g^{-1} after the first cycle, 11.760 mmol g^{-1}, after the second cycle and 11.630 mmol g^{-1} after the third cycle. Desorption of the Cu complex onto TCPP-SBA-15 was monitored by UV–vis spectroscopy (Fig. 7a). The UV–vis spectra of Cu-free TCPP-SBA-15 include two major features: a series of visible bands (Q-bands) and an extremely intense band (Soret band). Similar to the spectra of most free-base tetrakis(4-carboxyphenyl)porphyrin, that of Cu-free TCPP-SBA-15 shows well-defined Q bands that are assigned to the $0 \rightarrow 0$ and $0 \rightarrow 1$ vibronic transitions of the distinct x and y components of the lowest $\pi \rightarrow \pi^*$ transition. This proves that Cu(II) was recovered during the desorption process. The spectrum of the reused adsorbent shows bands similar to those in the spectrum of Cu-tetrakis(4-carboxyphenyl)porphyrin, which also has a Soret band at 417 nm and Q-bands at 540 and 583 nm (Fig. 7a). To confirm the presence of Cu(II) ions inside TCPP-SBA-15, we performed EPR studies on TCPP-SBA-15 samples containing adsorbed Cu(II) ions (Fig. 7b). The EPR spectrum of the TCPP-SBA-15 samples containing adsorbed Cu(II) ions can be explained in terms of an axial spin Hamiltonian with parameters $g_{||} = 2.20$ and $g_{\perp} = 2.06$, which indicates that the Cu(II) ions linked to nitrogen ligands in TCPP have a square planar symmetry (Fig. 7b) [28].

4. Conclusion

The adsorption of Cu(II) ions on tetrakis(4-carboxyphenyl)porphyrin (TCPP)-functionalized NH_2-SBA-15 was investigated. Metal adsorption on TCPP-SBA-15 was carried out using different initial concentrations of Cu(II). The maximum adsorption of Cu(II) on the TCPP-SBA-15 sample was 12.96 mmol of Cu(II) per gram of the adsorbent. The desorption process reached equilibrium at 60 min and the desorption rate for Cu(II) was 65.1%. Regeneration experiments carried out for TCPP-SBA-15 containing adsorbed Cu(II) ions revealed that the adsorption capacities were around 11.906, 11.760, and 11.630 mmol g^{-1} after three successive adsorption–desorption cycles. Thus, we can conclude that TCPP ligands enable these materials to function as adsorbents for the removal of Cu(II) ions.

References

[1] X. Ying, Z. Fang, Experimental research on heavy metal wastewater treatment with dipropyl dithiophosphate, J. Hazard. Mater. 137 (2006) 1636–1642.
[2] M.M. Matlock, B.S. Howerton, K.R. Henke, D.A. Atwood, A pyridine-thiol ligand with multiple bonding sites for heavy metal precipitation, J. Hazard. Mater. 82 (2001) 55–63.
[3] E. Malkoc, Y. Nuhoglu, Investigations of nickel(II) removal from aqueous solutions using tea factory waste, J. Hazard. Mater. 127 (2005) 120–128.
[4] J. Yan, R. Wang, M. Wang, The fundamental principles and ecotechniques of wastewater aquaculture, Ecol. Eng. 10 (1998) 191–208.
[5] S. Veli, B. Alyüz, Adsorption of copper and zinc from aqueous solutions by using natural clay, J. Hazard. Mater. 149 (2007) 226–233.
[6] Y. Benito, M.L. Ruíz, Reverse osmosis applied to metal finishing wastewater, Desalination 142 (2002) 229–234.
[7] T.A. Kurniawan, G.Y.S. Chan, W.-H. Lo, S. Babel, Physico-chemical treatment techniques for wastewater laden with heavy metals, Chem. Eng. J. 118 (2006) 83–98.
[8] T. Mohammadi, A. Moheb, M. Sadrzadeh, A. Razmi, Modeling of metal ion removal from wastewater by electrodialysis, Sep. Purif. Technol. 41 (2005) 73–82.
[9] A. Oehmen, R. Viegas, S. Velizarov, M.A.M. Reis, J.G. Crespo, Removal of heavy metals from drinking water supplies through the ion exchange membrane bioreactor, Desalination 199 (2006) 405–407.
[10] T.J. Butter, L.M. Evison, I.C. Hancock, F.S. Holland, K.A. Matis, A. Philipson, A.I. Sheikh, A.I. Zouboulis, The removal and recovery of cadmium from dilute aqueous solutions by biosorption and electrolysis at laboratory scale, Water Res. 32 (1998) 400–406.
[11] K. Kadirvelu, K. Thamaraiselvi, C. Namasivayam, Removal of heavy metals from industrial wastewaters by adsorption onto activated carbon prepared from an agricultural solid waste, Bioresour. Technol. 76 (2001) 63–65.
[12] A. Sarl, M. Tuzen, M. Soylak, Adsorption of Pb(II) and Cr(III) from aqueous solution on Celtek clay, J. Hazard. Mater. 144 (2007) 41–46.
[13] S. Sönmez, U. Divrikli, L. Elçi, New use of polypyrrole-chloride for selective preconcentration of copper prior to its determination of flame atomic absorption spectrometry, Talanta 82 (2010) 939–944.
[14] R.I. Nooney, M. Kalyanaraman, G. Kennedy, E.J. Maginn, Heavy metal remediation using functionalized mesoporous silicas with controlled macrostructure, Langmuir 17 (2000) 528–533.
[15] L. Mercier, T.J. Pinnavaia, Heavy metal ion adsorbents formed by the grafting of a thiol functionality to mesoporous silica molecular sieves: factors affecting Hg(II) uptake, Environ. Sci. Technol. 32 (1998) 2749–2754.
[16] X. Feng, G.E. Fryxell, L.-Q. Wang, A.Y. Kim, J. Liu, K.M. Kemner, Functionalized monolayers on ordered mesoporous supports, Science 276 (1997) 923–926.
[17] A. Walcarius, C. Delacote, Rate of access to the binding sites in organically modified silicates. 3. Effect of Structure and density of functional groups in mesoporous solids obtained by the Co-condensation route, Chem. Mater. 15 (2003) 4181–4192.
[18] K. Cassiers, T. Linssen, M. Mathieu, M. Benjelloun, K. Schrijnemakers, P. Van Der Voort, P. Cool, E.F. Vansant, A detailed study of thermal, hydrothermal, and

mechanical stabilities of a wide range of surfactant assembled mesoporous silicas, Chem. Mater. 14 (2002) 2317–2324.
[19] X. Xue, F. Li, Removal of Cu(II) from aqueous solution by adsorption onto functionalized SBA-16 mesoporous silica, Micropor. Mesopor. Mater. 116 (2008) 116–122.
[20] K.F. Lam, C.M. Fong, K.L. Yeung, G. McKay, Selective adsorption of gold from complex mixtures using mesoporous adsorbents, Chem. Eng. J. 145 (2008) 185–195.
[21] K.F. Lam, K.L. Yeung, G. McKay, A rational approach in the design of selective mesoporous adsorbents, Langmuir 22 (2006) 9632–9641.
[22] R. Hanzel, P. Rajec, Sorption of cobalt on modified silica gel materials, J. Radioanal. Nucl. Chem. 246 (2000) 607–615.
[23] S.p. Goubert-Renaudin, M. Etienne, S.p. Brandeѐ, M. Meyer, F. Denat, B.n.d. Lebeau, A. Walcarius, Factors affecting copper(II) binding to multiarmed cyclam-grafted mesoporous silica in aqueous solution, Langmuir 25 (2009) 9804–9813.
[24] D.W. Thomas, A.E. Martell, Metal chelates of tetraphenylporphine and of some p-substituted derivatives1,2, J. Am. Chem. Soc. 81 (1959) 5111–5119.
[25] Sujandi, S.-E. Park, D.-S. Han, S.-C. Han, M.-J. Jin, T. Ohsuna, Amino-functionalized SBA-15 type mesoporous silica having nanostructured hexagonal platelet morphology, Chem. Commun. (2006) 4131–4133.
[26] H. Yang, R. Xu, X. Xue, F. Li, G. Li, Hybrid surfactant-templated mesoporous silica formed in ethanol and its application for heavy metal removal, J. Hazard. Mater. 152 (2008) 690–698.
[27] L.D. White, C.P. Tripp, Reaction of (3-aminopropyl)dimethylethoxysilane with amine catalysts on silica surfaces, J. Colloid Interface Sci. 232 (2000) 400–407.
[28] A. Poppl, M. Hartmann, L. Kevan, Electron spin resonance and electron spin echo modulation studies of Cu(II) ion coordination and adsorbate interaction in ion-exchanged AlMCM-41 mesoporous materials, J. Phys. Chem. 99 (1995) 17251–17258.